

Supplementary Information

A Dual Function Electro-Optical Silicon Field-Effect Transistor Molecular Sensor

Pradhana Jati Budhi Laksana^{1,2,3}, Li-Chu Tsai^{4,*}, Tsai-Yin Wei^{4,5}, Pei-Chi Lan^{3,4}, Kuei-Shu Chang-Liao¹, Mathew K. Moodley⁶, and Chii-Dong Chen^{3,*}

Si-FET is a device that the current flow from source to drain is controlled by the electric field defined by the gate electrode. When used as a biosensor, the molecules attached on the FET channel surface play the role of the top gate, in which the molecular charges produce an electrical field that modulate the FET current. Upon molecular interaction, the absorption of photons of a specific wavelength is changed. Consequently, the photon intensity changes and can be detected by using the FET. In this way, the FET can detect both molecular charge and molecular absorption.

A. Details of the device fabrication

Silicon FET Sensor were fabricated using top down technology on a 6 in. silicon on insulator (SOI) wafer of 375 nm oxide and 100 nm top silicon. The top silicon layer was n-type doped with phosphorus for a concentration of $1 \times 10^{11} \text{ cm}^{-2}$ and energy of 20 keV to create accumulation-mode FET. Dopant activation was followed using rapid thermal annealing (RTA) in 1000 °C for 20 s. This layer was etched using conventional optical lithography and inductively-coupled plasma reactive-ion etching (ICP-RIE) to define the active region including the source/drain and nanowire. For gate oxide, 15 nm silicon oxide was grown using wet oxidation furnace at 900 °C. A deposition of 150 nm polysilicon process was followed at active area to protect for following process. Additional source and drain doping was performed with arsenic for a concentration of $1 \times 10^{14} \text{ cm}^{-2}$ to reduce contact resistance of the source/drain region, followed using RTA in 1000 °C for 20 s.

Interlayer dielectric (ILD) then was formed to prevent the crosstalk to adjacent metal lines. An evaporated metal stack of 800 nm aluminum on 150 nm titanium was defined using the lift-off process for source/drain line. The source/drain line then were passivated by silicon oxide and nitride to avoid direct connection to the sample solution.

B. FET measurement setup

Electrical measurement of FET device was measured using a custom-made data acquisition system connected to a computer running an in-house software written with Lab-VIEW (National Instruments, USA). The sensor assembly accommodates an FET chip with fluidic channels and an optical fiber adapter, was connected to the acquisition platform by an HDMI cable. The specimen solution is injected into the FET sensing area through a fluidic channel where the solution inlet and outlet are located at the two sides of the sensor assembly. The flow rate of the specimen solution is controlled by an HPLC pump (Pharmacia LKB P-500). An Ag/AgCl reference electrode was inserted into the fluidic channel to maintain a fixed electrolyte potential of the liquid gate. The light source consists of a Xenon fiber optic light source (ASB-XE-175EX, Spectral Products) and a monochromator (CM110, Spectral Products). Light is introduced onto the FET sensing area from the top of the sensor assembly. In this acquisition system, the user allows to control the measurement parameter such as the drain voltage, back-gate voltage, liquid-gate voltage, light intensity, wavelength, and time.

C. Device characteristics

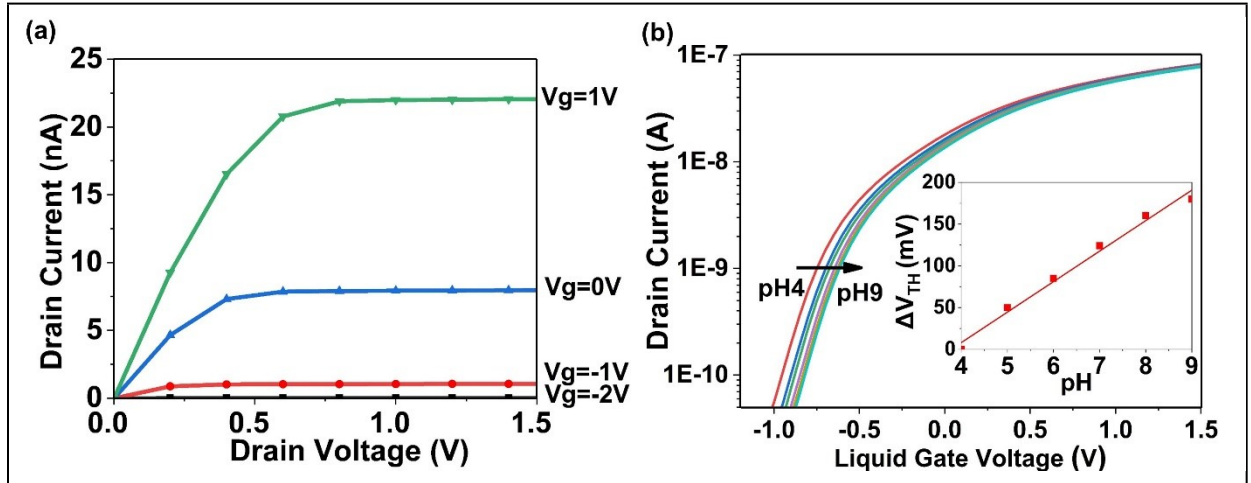


Figure S1. Basic characterization of FET: (a) Output characteristics of the silicon FET sensor and (b) pH sensitivity response of the FET device ranging from pH 4 to pH 9. The bias condition V_{DS} 0.5 V, V_{LG} -1 V to 1.5 V, and V_{BG} was kept constant at 0 V.

To characterize the sensitivity of different pH, the measurement of $I-V_{LG}$ was screened under different pH ranging from 4-9 (Figure S1). The threshold voltage V_{TH} is defined as the gate voltage at drain current of 1nA ¹. Typically, the devices displayed a subthreshold swing of 215 mV per decade and an on/off current ratio of about $1e5$. The results showed that the response of the FET chip to pH was indeed highly linear with a linear fit r-square value of 0.98823. The slope of the fitting line represents the sensitivity to pH with the value of 45 mV pH^{-1} . The sensitivity of pH in this device is lower than the Nernst limit (59 mV pH^{-1}). This different might be due to the high electrolyte screening², protonation affinity of the sensor surface, and finite semiconductor capacitance³.

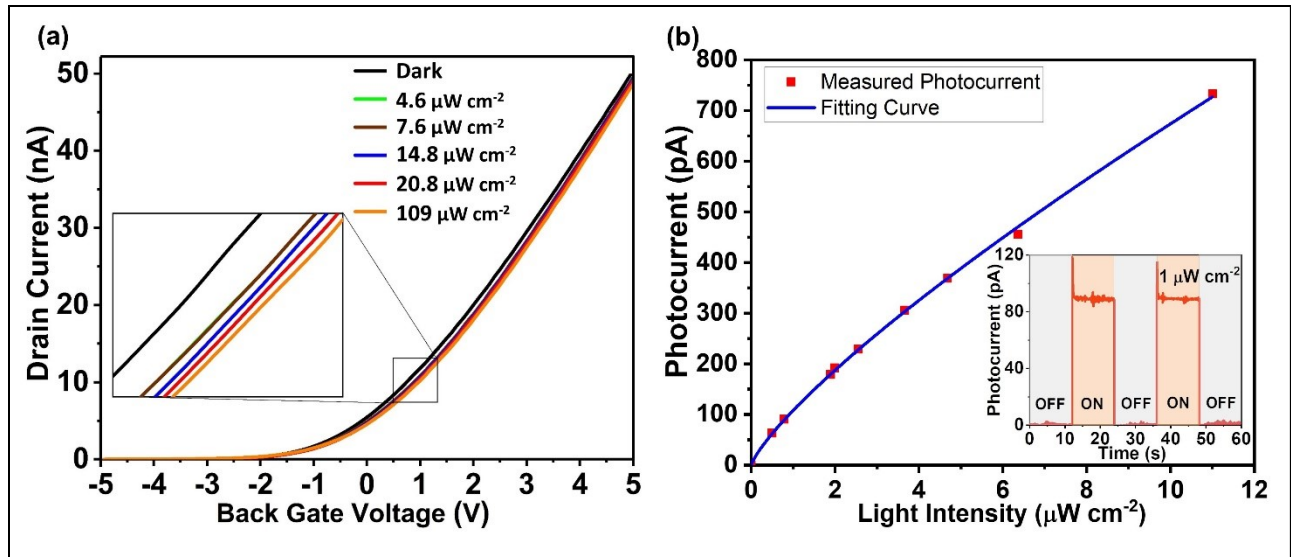


Figure S2. In (a) I_{DS} - V_{BG} response of the FET under various levels of light illumination: dark (black), 4.6 (green), 7.6 (brown), 14.8 (blue), 20.8 (red) and 109 (orange) $\mu\text{W cm}^{-2}$ with bias condition V_{DS} 0.5 V, V_{BG} -5 V to 5 V, and V_{LG} was kept constant at 0V. The current at all back-gate voltage decreases with increasing light intensity. In (b) red dots are measured photocurrent, and the black curve is the power-law fitting. The inset shows on/off photocurrent under 1 $\mu\text{W cm}^{-2}$ light intensity. Photocurrent increases sub linearly and follows power-law dependence for light intensity below 11 $\mu\text{W cm}^{-2}$.

The photocurrent characteristics measured with bias condition V_{DS} 0.5 V, V_{BG} -5 V to 5 V, V_{LG} was kept constant at 0 V and fix wavelength 650 nm for varying light intensity is shown in Figure S2a. The current at all back-gate voltage decreases with increasing light intensity. The absolute photocurrent then plotted under different light intensity at V_{BG} 0 V. Enhancement in light intensity leads to an increase in device photocurrent. However, the photocurrent increases sub linearly with excitation power. The experimental data was fitted using a power-law dependent I_{ph} (μA) = 6.34 $A^{0.794}$ (Figure S2b).

D. Real-time measurement of NGAL

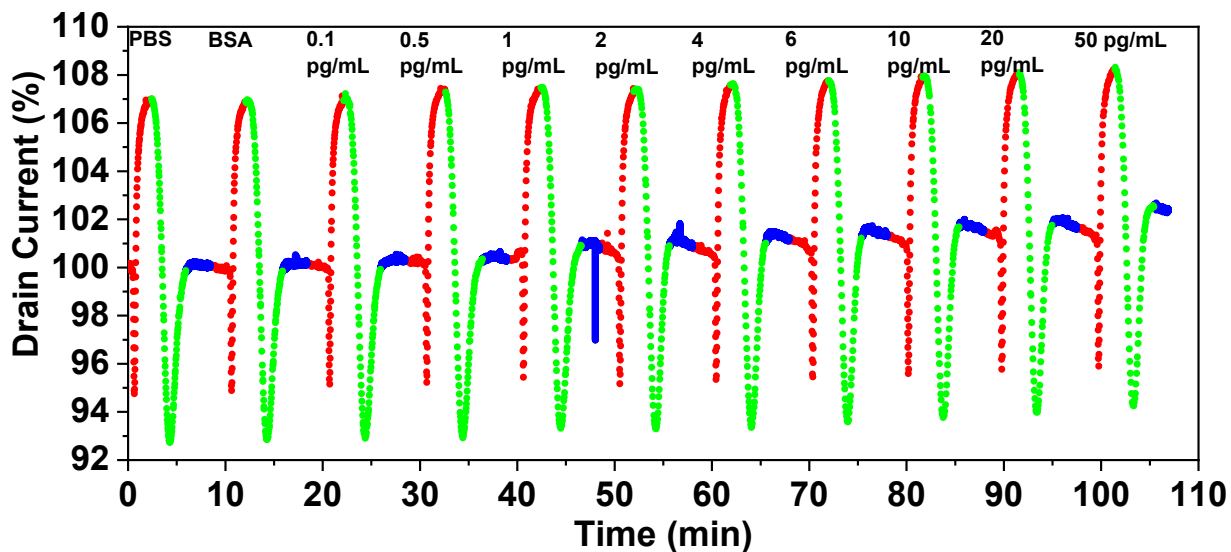


Figure S3. The real-time FET response to different concentration of NGAL ranging from 0.1 to 50 pg mL^{-1} .

The real-time FET response to different NGAL concentrations is shown in Figure S3. The measurement was performed under a constant flow rate of 7 ml/h. During the time period shown in red dots, the NGAL solution was injected. This was then followed by injection of buffer solution (shown in green dots) to wash away the unbound NGAL. After washing, only the bounded NGAL molecules remain on the FET surfaces, and the averaged FET current during the period of blue dots was then taken and shown in Figure 5 of the main text. Upon injection of NGAL solution (red dots), the surface ion concentration of the electrical double layer on the FET surface first decreased abruptly because of the solution turbulence, and then increased exponentially with time, resulting in a sharp drop and increase of the FET current. Similar behaviour was observed also for buffer solution, shown in green dots. The detection of NGAL binding was taken only when the current stabilized after removing of unbound NGAL by buffer solution. The first two blue traces have the same current height because there were no NGAL bindings and there were sets as reference currents to 100%. With increases NGAL concentration, the current in percentage increases. In

Figure S4, we show the IV_{BG} characteristics taken in the beginning and the end of the I-time measurement.

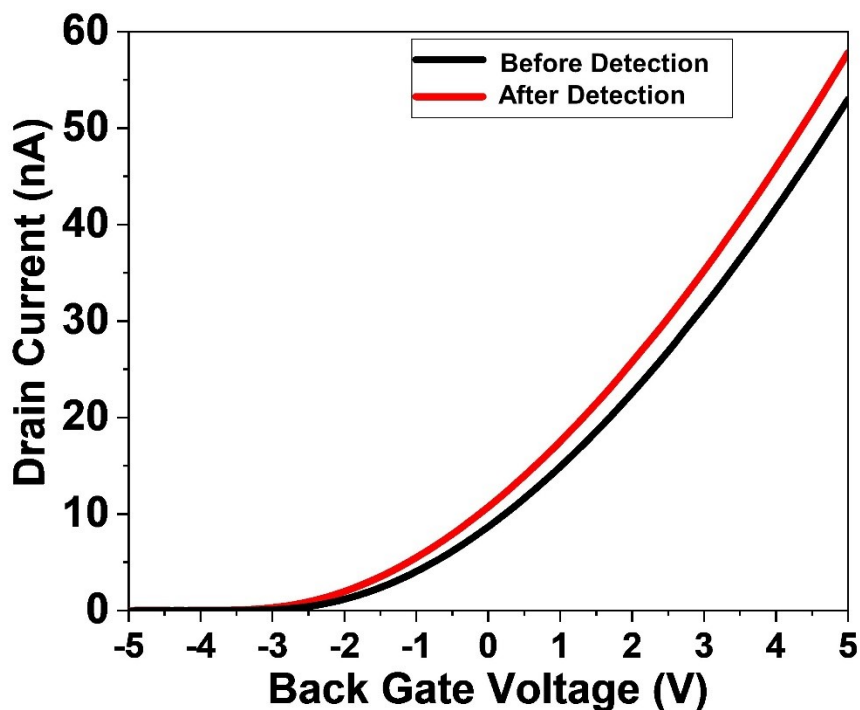


Figure S4. The FET current as a function of the back gate voltage taken before (black) and after (red) the measurement shown in Figure S3.

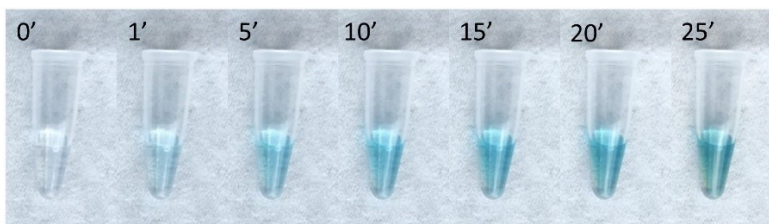


Figure S5. The color evolution of oxidized TMB for 50 pg mL^{-1} NGAL at different time in minutes.

Figure S5 shows the color evolution oxidized TMB for 50 pg mL^{-1} NGAL. It shows gradually change of the color from transparent to dark blue, indicating the increasing concentration of oxidized TMB.

References

1. A. Ortiz-Conde, F. J. García Sánchez, J. J. Liou, A. Cerdeira, M. Estrada and Y. Yue, *Microelectronics Reliability*, 2002, **42**, 583-596.
2. P. R. Nair and M. A. Alam, *Nano letters*, 2008, **8**, 1281-1285.
3. L. Bousse, N. F. D. Rooij and P. Bergveld, *IEEE Transactions on Electron Devices*, 1983, **30**, 1263-1270.